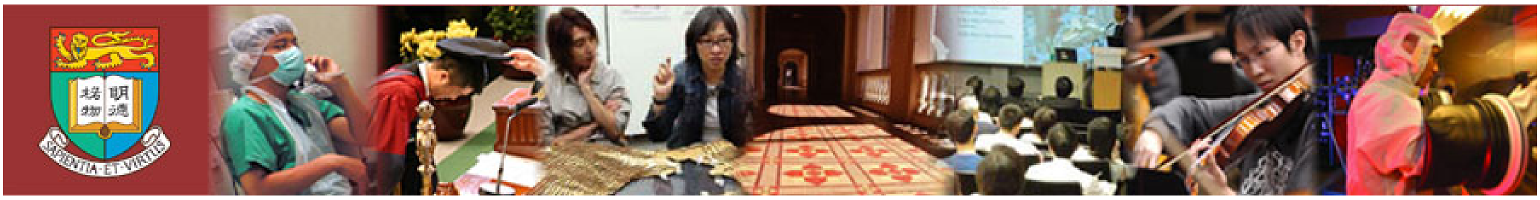

A Dual-Mode Dual-Band Ring Resonator Bandpass Filter with Controllable In-Between Isolation

Sheng Sun

Department of Electrical and Electronic Engineering, The University of Hong Kong, Pokfulam Road, Hong Kong
Email: sunsheng@ieee.org

***Abstract* — In this paper, a dual-mode dual-band bandpass filter with controllable in-between isolation is presented using a single microstrip ring resonator. By installing two dispersion-controlled coupled-line sections on the ring resonator at the two ports with 90°-separation, two transmission poles can be easily emerged and distributed in each passband. Meanwhile, two transmission zeros are generated between the two passbands, which can be used to control the rejection level of the in-between isolation. Instead of perturbing the gap distance between one of the open ends of the coupled-line section and the ring, a pair of open-circuited stubs is further installed along the symmetrical plane of the ring resonator, which can effectively enlarge the tuning range of the two transmission zeros. A prototype dual-band filter is finally designed, fabricated, and verified through the experiment.**

***Index Terms* — Bandpass filters, dual-band, dual-mode, isolation, ring resonators.**

I. Introduction

Multi-band bandpass filters have been extensively studied for the design of the multi-band radio frequency (RF) and microwave wireless communication systems. In order to satisfy the diversified spectrum requirements for the different communication devices, the front-end module is always preferred to have a compact size and the multi-band functions. In other words, it is expected that the design parameters of a multi-band filter, such as the fractional bandwidths (FBWs), the locations of multiple operating frequencies, the rejection skirts, as well as isolations, could be well controlled. Recently, the dual- and triple-band bandpass filters using a single ring resonator have been reported [1]-[4]. A set of two degenerate modes of a ring resonator have been excited and utilized to realize two separable transmission poles in each passband.

For the dual-band filters, the ratio between the second and the first operating frequencies (f_2/f_1) can be adjusted by either installing tuning stubs along the ring [1] or using a step-impedance shaped transmission line [5]. However, the tuning of these frequency ratios becomes complicated and even more difficult if more than two operating passbands are desired for those filters using only a single ring resonator. Especially, the in-between isolation becomes more important if the two passbands are close to each other, e.g., when $f_2/f_1 < 2$. It implies that at least two transmission zeros should be generated to control the rejection level between two passbands. In our recent work [6], two identical coupled-line sections are attached on the ring resonator at the two ports with 90°-separation. In this way, two degenerate modes can be easily excited to construct two transmission poles for each passband, where the ratio of two operating frequencies (f_2/f_1) for the uniform ring resonator is smaller than 2. By adjusting the small capacitive-coupled gap between one of the open ends of coupled-line section and the ring, the rejection level of in-between isolation can be tuned. When the two zeros are close to each other, the rejection level becomes higher, while the sharper rejection skirts require the two zeros far away from each other. However, the range of this tuning is restricted by the realizable distance of the gap.

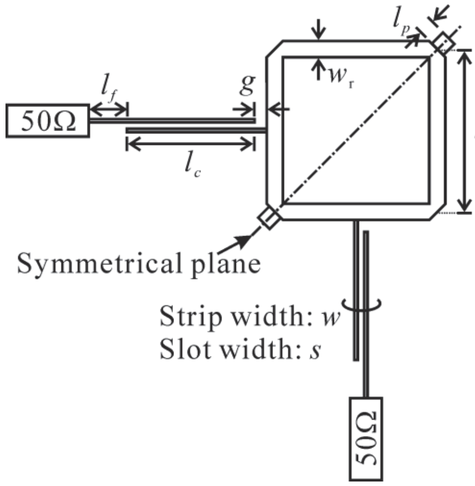

Fig.1. (a) Schematic of the proposed dual-band ring-resonator bandpass filter with varied perturbation stub length (l_p) and gap distances (g).

In this paper, in order to enhance the tuning ability of the in-between isolation, the two identical open-circuited shunt stubs are further installed along the symmetrical plane of the ring resonator, as shown in Fig. 1. By increasing the length of the perturbation stubs, the distance of the in-between two transmission zeros can be further enlarged. That means shaper rejection skirts can be achieved rather than those of using only gap perturbations. A prototype filter is designed and fabricated. The measured results agree well with those obtained from the *ADS Momentum* full-wave simulator [7].

II. Dual-Mode Dual-Band Filter Design

Fig. 1 shows the physical schematic of the proposed dual-band ring resonator bandpass filter. It consists of a single

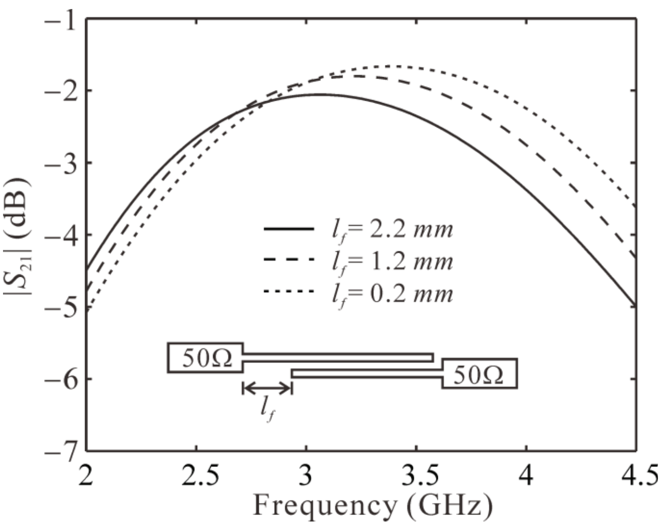

Fig.2. Magnitudes of the transmission coefficient ($|S_{21}|$) for the different extended length l_f.

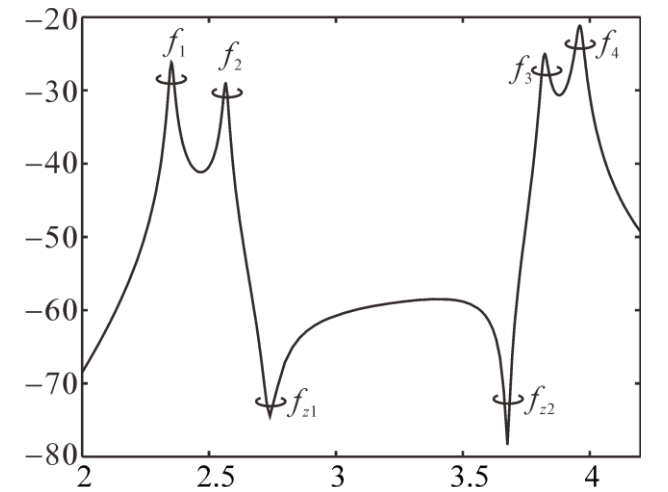

Fig. 3 Frequency responses of the proposed ring resonator under the weak coupling.

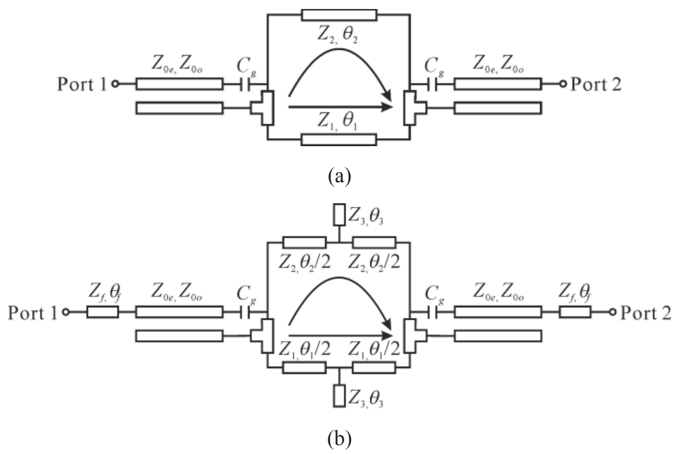

Fig. 4. Equivalent circuit model with lumped capacitor (C_g). (a) Without loading perturbation stubs. (b) With loading perturbation stubs.

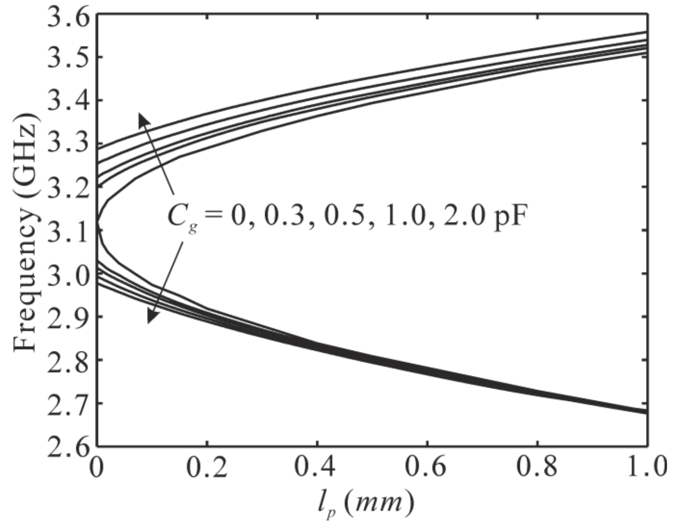

Fig.5. Frequency locations of the transmission zeros versus the length of perturbation stubs (l_p) under different lumped capacitors (C_g).

open-stubs-loaded resonator and two identified coupled-line sections. One of coupled-line arms can be extended to obtain the controlled dispersions in both two passbands. As shown in Fig. 2, the length of the extension, l_f, can be varied to achieve the different transmission strengths over the concerned frequencies. As l_f increases, the magnitude of the transmission coefficients ($|S_{21}|$) can be shifted to the lower frequencies and becomes smaller. In other words, the coupling at the left and the right sides of the coupling peak (the maximum of $|S_{21}|$) can be varied to be either smaller or larger, in order to arrange the necessary couplings in both two passbands.

To obtain two transmission poles in both two passbands, at least two degenerate modes should be excited in each passband. As discussed in [6], by stretching the length of stubs (one strip of coupled-line sections), the two first-order degenerate modes (at f_1 and f_2) were excited to form the first passband, while the second passband was constructed by the second-order degenerate mode at f_3 and one of the third-order degenerate modes at f_4 . In other words, as l_c increases, the two first-order degenerate modes shift down and away from their initial locations in-between the two zeros, while the other two higher-order degenerate modes shift down quickly and construct quasi-symmetric responses about the zeros. As shown in Fig. 3, two pairs of the degenerate modes of the ring resonator can be properly arranged around 2.5 and 3.9 GHz, respectively, while the two transmission zeros are generated between two operating frequencies at f_{z1} and f_{z2}.

Fig. 4 shows the equivalent circuit model for the dual-band ring resonator bandpass filters without and with the loaded perturbation stubs. Z_i and θ_i indicate the impedances and the electrical lengths of the single transmission line section, while the even-mode and odd-mode impedances of the coupled-line sections are denoted by Z_{0e} and Z_{0o}, respectively. In addition, the effect of the end-to-side coupling is approximately modeled by a simple series lumped capacitor, C_g. From the circuit topology point of view, the T-junction is also considered to identify the upper and lower transmission paths.

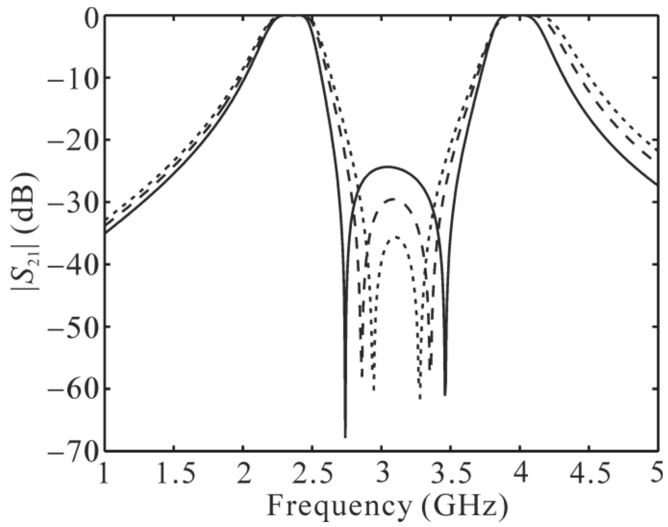

(a)

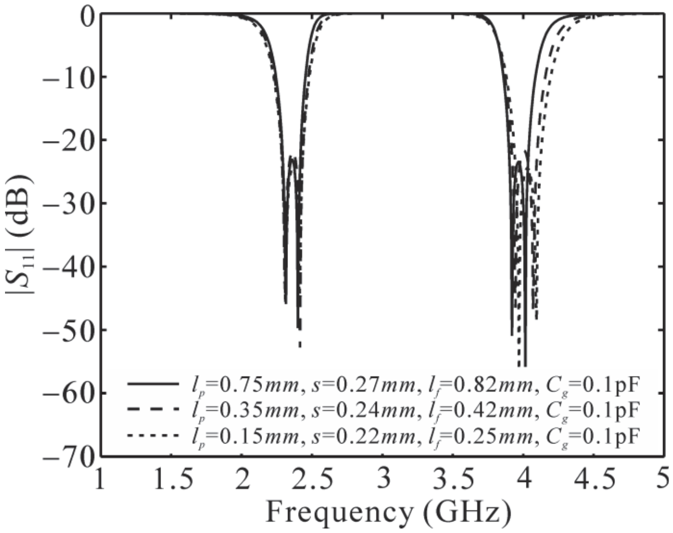

(b)

Fig.6. *S*-magnitudes of the proposed dual-band filters with different isolation level. (a) Magnitudes of the transmission coefficients ($|S_{21}|$). (b) Magnitudes of the reflection coefficients ($|S_{11}|$).

Obviously, the resonator in Fig. 4(a) can be considered as a special case of the one in Fig. 4(b), if the length of the loaded perturbation stubs are equal to zero (l_p = 0). Fig. 5 plots the frequency locations of the two transmission zeros versus the length of perturbation stubs under different C_g. These simulated results are obtained from the *ADS Schematic* circuit simulator [7]. Without considering the gap coupling (C_g = 0 pF) and the perturbation stubs (l_p), the two transmission zeros are overlapped at 3.12 GHz. As l_p is increased from 0 to 1.0 *mm* when C_g = 0, two transmission zeros are away from each other and reach 2.67 and 3.53 GHz, respectively, where the ratio of two zero frequencies is about 1.32. If C_g is increased, it is found that the lower zero (f_{z1}) is shifted down and the upper zero (f_{z2}) is shifted up. For higher frequencies, the

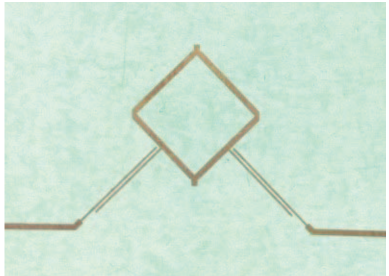

(a)

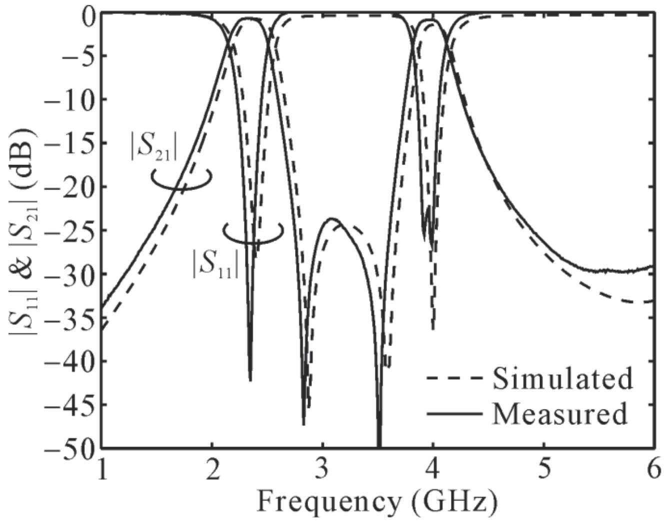

(b)

Fig.7. (a) Photograph of the fabricated dual-band dual-mode ring resonator bandpass filter. Dimensions: l_c= 8.8, w = 0.2, s = 0.24, g = 0.2, l_f = 1.49, l_r = 9, l_p = 0.65, unit: *mm*. Substrate: RT/Duroid 6010 with h = 0.635 *mm* and ε_r = 10.8. (b) Simulated and measured *S*-magnitudes. (b) Simulated and measured *S*-magnitudes.

wavelength of the standing wave along the ring is shorter. Therefore, the end-to-side coupling of the gap has more influence on the frequency variation of the upper zero, as shown in Fig. 5.

On the other hand, the varied lengths of the perturbation stubs along the symmetrical plane also affect the even-mode resonant frequencies when the even- and odd-mode analysis is applied [8]. Therefore, the coupling degree for each passband has to be adjusted accordingly, by adjusting the slot width of the coupled line (s) and the aforementioned extension with the line length of l_f. As shown in Fig. 6, three different rejection levels of isolation can be obtained from 35.6, 29.5, to 24.4 dB, where s and l_f have been optimized to achieve proper couplings and small in-band reflection (< 20 dB) in both two passbands.

Note that the ring resonator presented in this work involves two transmission paths with different electrical lengths. Both of C_g and l_p can be controlled to perturb the phase difference between these two paths, thus changing the locations of the phase cancellation and shifting the transmission zeros. Similar effect of the phase perturbation can also be achieved by changing the angle between input/output ports of the single band dual-mode filter [9].

III. Results and Discussion

To verify the performance of the above proposed structure, a prototype filter circuit is designed and optimized with dual passbands at 2.35 and 3.95 GHz in the *ADS Momentum* full-wave simulator [7]. Fig. 7(a) shows the photograph of the fabricated circuit. Fig. 7(b) shows its frequency responses over a wide frequency range from 1.0 to 6.0 GHz. The measured results show a good agreement with those obtained from the simulation. The measured minimum insertion loss achieves 0.7 dB in the first passband and 0.9 dB in the second passband. As predicted, two transmission zeros are observed at 2.83 and 3.51 GHz, respectively, which also results in a 23.7-dB isolation from 2.74 to 3.62 GHz.

IV. Conclusion

In this paper, a dual-band bandpass filter using a single open-stub-loaded microstrip ring resonator has been presented. The two transmission poles are generated in each passband after installing two coupled-line sections at two excitation ports. It has been shown that the tuning of two transmission zeros becomes more flexible after loading the perturbation elements along the symmetrical plane of the ring resonator. Good isolation has been achieved experimentally for the dual-band filter with $f_2/f_1 = 1.68$.

Acknowledgement

This work was supported by the Seed Funding Programme for Basic Research, The University of Hong Kong (Project No.: 201101159011).

References

[1] S. Luo and L. Zhu, “A novel dual-mode dual-band bandpass filter based on a single ring resonator,” *IEEE Microw. Wireless Compon. Lett.,* vol. 19, no. 8, pp. 497–499, Aug. 2009

[2] S. Luo, L. Zhu, and S. Sun, "A dual-band ring-resonator bandpass filter based on two pairs of degenerate modes," *IEEE Trans. Microw. Theory Tech.*, vol. 58, no. 12, pp. 0-1, Dec. 2010.

[3] Y.-C. Chiou, C.-Y. Wu, and J.-T. Kuo, “New miniaturized dual-mode dual-band ring resonator bandpass filter with microwave C-sections,” *IEEE Microw. Wireless Compon. Lett*, vol. 20, no. 2, pp. 67–69, Feb. 2010.

[4] S. Luo, L. Zhu, and S. Sun, “Compact dual-mode triple-band bandpass filters using three pairs of degenerate modes in a ring resonator,” *IEEE Trans. Microw. Theory Tech.*, vol. 59, no. 5, pp. 1222-1229, May 2011.

[5] T.-H. Huang, H.-J. Chen, C.-S. Chang, L.-S. Chen, Y.-H. Wang, and M.-P. Houng, “A novel compact ring dual-mode filter with adjustable second-passband for dual-band applications,” *IEEE Microw. Wireless Compon. Lett.*, vol. 16, no. 6, pp. 360–362, Jun. 2006.

[6] S. Sun, “A dual-band bandpass filter using a single dual-mode ring resonator,” *IEEE Microw. Wireless Compon. Lett*, vol. 21, no. 6, pp. 298-300, Jun. 2011.

[7] Advanced Design System (ADS), Agilent Technol., Palo Alto, CA.

[8] S. Sun and L. Zhu, “Wideband microstrip ring resonator bandpass filters under multiple resonances,” *IEEE Trans. Microw. Theory Tech.*, vol. 55, no. 10, pp. 2176-2182, Oct. 2007.

[9] A. C. Kundu and I. Awai, “Control of attenuation pole frequency of a dual-mode microstrip ring resonator bandpass filter,” *IEEE Trans. Microw. Theory Tech.*, vol. 49, no. 6, pp. 1113-1117, Jun. 2001.